



**HAL**  
open science

# Biologically-Inspired Visual Scanning Sensor for Stabilization and Tracking

S. Viollet, N. Franceschini

► **To cite this version:**

S. Viollet, N. Franceschini. Biologically-Inspired Visual Scanning Sensor for Stabilization and Tracking. IEEE/RSJ International Conference on Intelligent Robots and Systems (IROS'99), Sep 1999, Kyongju, South Korea. pp.204-209, 10.1109/IROS.1999.813005 . hal-03844369

**HAL Id: hal-03844369**

**<https://amu.hal.science/hal-03844369>**

Submitted on 14 Nov 2022

**HAL** is a multi-disciplinary open access archive for the deposit and dissemination of scientific research documents, whether they are published or not. The documents may come from teaching and research institutions in France or abroad, or from public or private research centers.

L'archive ouverte pluridisciplinaire **HAL**, est destinée au dépôt et à la diffusion de documents scientifiques de niveau recherche, publiés ou non, émanant des établissements d'enseignement et de recherche français ou étrangers, des laboratoires publics ou privés.

## Biologically-Inspired Visual Scanning Sensor for Stabilization and Tracking

Stéphane Viollet and Nicolas Franceschini

C.N.R.S., Laboratoire de Neurobiologie, LNB3  
31, chemin Joseph Aiguier  
13402 Marseille Cedex 20, FRANCE  
[sviollet, enfranceschini]@lnb.cnrs-mrs.fr

### Abstract

*Here we describe a new sensor designed to ensure the non contact stabilization of a craft and especially to deal with disturbance problems such as those resulting from slow speed angular drift. A low-cost, low-complexity active vision system is described, which is based on the specific eye movements occurring in the compound eye of the fly. In our system, motion is detected and processed by a Local Motion Detector circuit (LMD). First, the rotation of two photosensors at a constant angular speed was simulated, which emphasized motion processing as a useful means of detecting variably contrasted objects, however far ahead they are located. Secondly, we reasoned that if the pair of photosensors turns at a varying angular speed, the signal delivered by the LMD will vary depending on the position of the contrast feature located in the sensor's visual field. The validity of this reasoning was then tested by constructing a miniature scanning sensor, the output voltage of which turned out to be a quasi-linear function of the position of the contrast feature present in the visual field and to be largely independent of the distance and the level of contrast. This output can therefore be used to generate the appropriate motor commands for stabilizing a sensory platform subject to yaw, pitch, or roll in relation to environmental features and/or for tracking contrasting objects.*

### 1. Introduction

The classical method for stabilizing a system (e.g., an aircraft) and preventing yaw, pitch and roll, consists of using a gyroscopic sensor. Gyroscopes tend, however, to drift depending on the time and temperature [10]. Other approaches involve the use of visual systems based on elaborate optical sensors and mathematical algorithms requiring large computational resources. Here we approach the problem of stabilization in relation to an

optical target (a contrast edge) in the center of the visual field, such as that solved by a hovering insect that tries to keep the image of an object at a particular point on its retina [1][2]. In the biologically-inspired visual sensor described here, which draws on the results of electrophysiological and behavioral studies recently carried out at our laboratory on the fly visual system [3], a method based on visual motion detection combined with scanning was successfully used to detect slow speed angular drift with respect to a stationary or slowly moving contrast feature. In order to perform visual tracking without requiring a CCD camera and digital processing, we used a hardware Local Motion Detection circuit (LMD), designed on similar lines to those on which the fly visual system is based [4][5]. The front end of an LMD consists of two photosensors having adjacent visual axes [11]. When a contrast edge moves past these adjacent photosensors, the LMD generates an output signal which is proportional to the angular speed  $\Omega$ , i.e., which is inversely proportional to the time  $\Delta t$  elapsing between the stimulation of the two photosensors. In essence, biological LMD's respond to *relative* movements between a living creature and its contrasting environment. When the eye of a creature undergoes a pure rotation, e.g., in yaw, within a stationary world, the angular speed of contrast features located at a given elevation remains constant, regardless of their distances [1]. In sections 1 and 2, we simulate the pure rotation of a single pair of adjacent pixels encountering a stationary contrast feature and show that the processing of the apparent motion by an LMD yields a robust response, regardless of the distance, orientation and level of contrast. In sections 3 and 4, we describe how an imposed, concerted rotation of the pair of photosensors at an angular speed which varies with time (*variable speed scanning*) generates an LMD signal with an interesting property: the signal generated varies with the angular *position* of a contrast feature located in the visual field. The present approach differs from two other

approaches that were recently based on the same biological findings:

- with the first approach, motion detectors driven by a retina scanning the environment at a *constant speed* enhanced the detection of slow relative angular velocities by the eye of a moving robot [8].

- with the second approach, a *pulse-scanning* mode involving no motion detectors was used to simply detect the presence of a contrast within the visual field [9].

Here, we demonstrated the efficiency and robustness of *variable speed scanning* combined with *motion detection* by constructing a small, low-cost optical scanning sensor. Upon varying the orientation of the sensor with respect to a stationary contrasting object, the output signal was found to vary quasi-linearly with the orientation of the sensor, regardless of the distance and the level of contrast involved.

## 2. Vision and rotational motion

### 2.1. Angular sensitivity

The angular sensitivity of an insect lens equipped with its photoreceptor is usually approximated by a bell-shaped function [6]. In the present case, we use a Gaussian function, the bottom part of which is truncated below the threshold  $s_0$ .

The angular sensitivity  $S(\varphi)$  of a photosensor  $i$  is therefore given by:

$$S(\varphi) = \left( \frac{\text{abs}(G_i(\varphi) - s_0) + (G_i(\varphi) - s_0)}{2} \right) \quad (1)$$

$$\text{with } G_i(\varphi) = \exp \left[ -\frac{\varphi^2}{2\sigma^2} \right] \quad (2)$$

The main parameters which characterize  $S(\varphi)$  are as follows :

- $L_v$  : total angular width of the visual field
- $\Delta\rho$  : angular width at half height

Both paramaters can be expressed with respect to  $\sigma$  as follows:

$$\Delta\rho = 2\sigma \left[ 2 \ln \left( \frac{2}{1+s_0} \right) \right]^{\frac{1}{2}} \quad (3)$$

$$L_v = 2\sigma \left[ 2 \ln \left( \frac{1}{s_0} \right) \right]^{\frac{1}{2}} \quad (4)$$

### 2.2. Scanning at a constant angular speed

As sketched in Figure 1, we simulated the concerted rotation of two photosensors, 1 and 2, separated by a constant angle  $\Delta\varphi$ , called the interreceptor angle, scanning a simplified landscape consisting of a single stationary segment, AB, having various grey values. The pair of photosensors is assumed here to rotate clockwise at a constant angular speed  $\Omega$ . The yaw angle  $\psi$  is given by

$$\psi(t) = \psi_o - \Omega t \quad (5)$$

The position of the segment is defined by the points  $A(x_1, y_1)$  and  $B(x_2, y_2)$  with  $y_1 = y_2$ . The width of the segment is  $l$  and  $x_2 = x_1 + l$ .

At any time, the output  $R_i(t)$  of a photosensor  $i$  can be obtained by integrating the angular sensitivity  $S(\varphi)$  weighted with the intensity  $I(\varphi)$ :

$$R_i(t) = \int_{-L_v/2}^{L_v/2} I(\varphi) S(\varphi) d\varphi \quad (6)$$

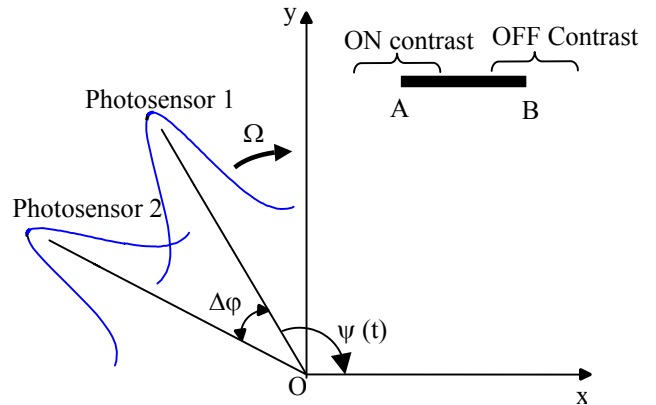


**Fig. 1** Rotation of the two photosensors separated by  $\Delta\varphi$ .

Segment AB is characterized by its grey level  $I$  (black = 10; white = 0). The grey level of the background is  $I = 0$ . All calculations and simulations were performed using custom-written programs using Matlab<sup>TM</sup>.

### 2.3. Processing the photoreceptor signals

To calculate the output signal from each photoreceptor, we used a discrete version of equation (6). The signal sampled,  $R_i(kT)$ , with  $T$  in seconds, results from a convolution of the light intensity  $I$  with the Gaussian mask  $S(kTs)$  ( $Ts$  in degrees). In other words, at each value of  $\psi$ ,  $R_i(kT)$  results from the filtering of  $I$  by a filter which has a Gaussian-shaped impulse response. In all these calculations, the Gaussian mask  $S(kTs)$  based on

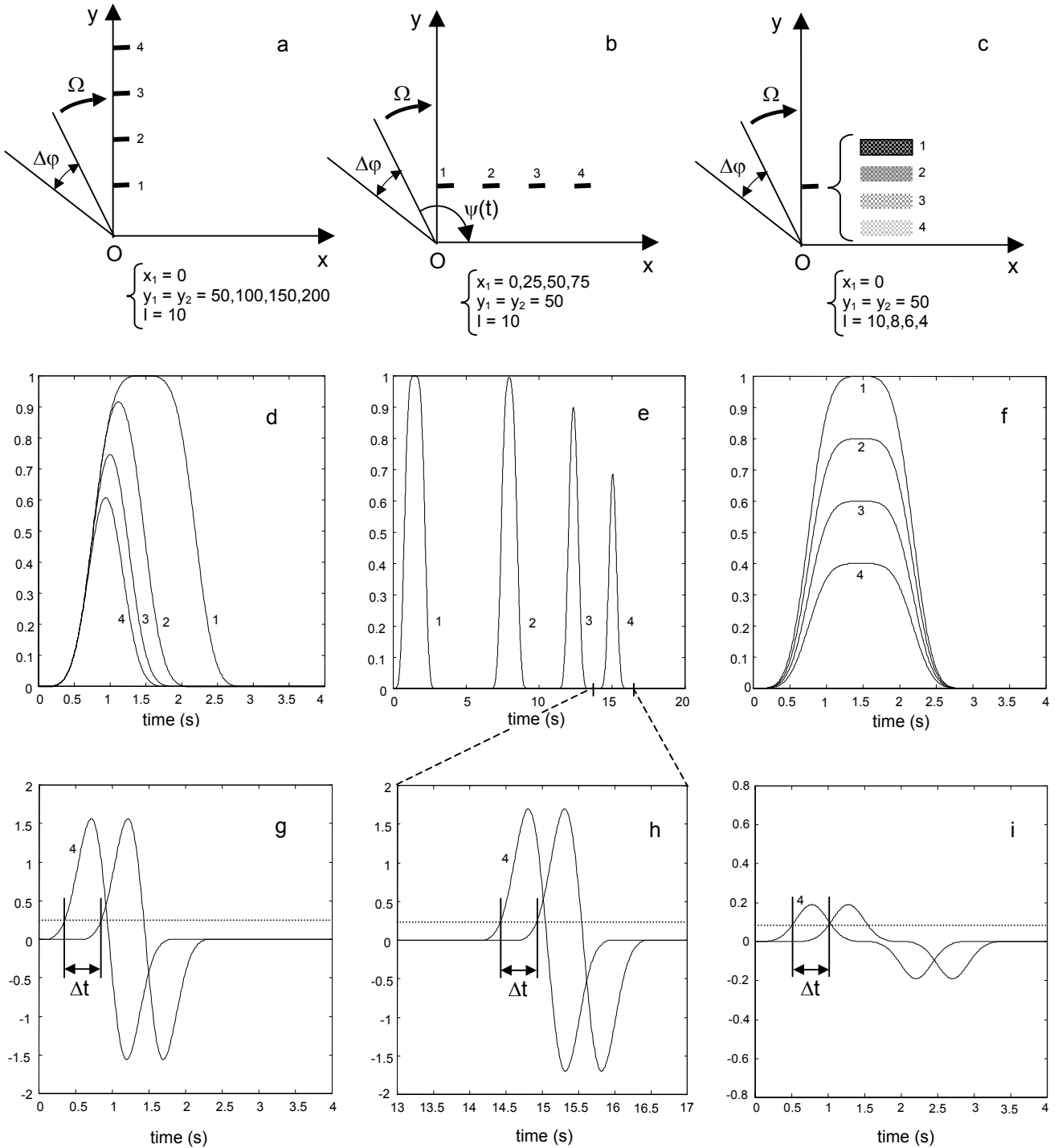


**Fig. 2** Simulated response of two adjacent photosensors rotating at an angular speed  $\Omega$ , encountering a black segment placed at various distances 1, 2, 3, 4 (a), and orientations (b), or which stays in the same position but displays various grey levels (c).

Figures 2d, 2e, 2f show the output from the photosensor 1.

Figures 2g, 2h, 2i show the derivative and thresholding of the output signal from each photosensor when the segment is in distance 4 (Figures 4g, 4h) or displays contrast level 4 (Figure 4i).

$\Delta\rho = 2^\circ$ ,  $\Delta\phi = 2^\circ$ ,  $L_V = 5.2^\circ$ ,  $s_0 = 0.01$ ,  $\Omega = 4^\circ/\text{s}$ ,  $l = 5$ ,  $T = 0.01\text{s}$

equation (1) was processed with a spatial sampling step  $T_s$  equal to  $0.004^\circ$ .  $R_i(kT)$  was normalized with respect to its extremal values:

- $R_i(kT) = 1$  when a segment with  $I = 10$  covers the whole visual field  $L_v$ .
- $R_i(kT) = 0$  when the segment is completely outside the visual field ( $I = 0$ ).

In order to test the robustness of the motion detection process, we examined three cases, as depicted in Figure 2 (a, b, c).

In the first case, we varied the distance of the segment along the y axis (Figure 2a). In the second case, we varied the position of the segment along the x axis (and hence its inclination with respect to the rotating photosensor pair) (Figure 2b). In the third case, we varied the contrast of the segment (Figure 2c) without changing its position. Figures 2(d,e,f) give the output from photosensor 1 in each of the three cases considered, as it turns clockwise at a constant angular speed  $\Omega$ . Figures 2(g,h,i) give the derivative of the output from each photosensor. In each of the three cases considered, we used Euler's method to compute a discrete derivative with sampling interval  $T$ . The use of the derivative in the first processing step is essential [7], as it makes it possible to :

- eliminate the DC level of the photosensors
- discriminate between positive (ON) contrasts and negative (OFF) contrasts (Figure 1).

#### 2.4. Time lag measurement as a robust processing step

Figures 2(g,h,i) show that processing the time elapsing between the thresholded temporal derivatives of each photoreceptor signal is a robust processing step for the detection of motion because at a constant angular speed  $\Omega$ , the time lag  $\Delta t$  measured between these processed signals remains invariant with respect to the distance, inclination and grey level of the segment. Only the amplitude of the derivative is affected by these variations.

### 3. Local Motion Detector

The analog motion detector is an analog optronic circuit that mimicks the fly motion detecting neurons [4]. Its graded output (in Volts) is inversely proportional to the time lag  $\Delta t$  discussed above, and hence approximately proportional to the angular speed  $\Omega$ . The photosensor output is processed by a passive high-pass filter and then by an active low-pass filter. After thresholding this filtered output, the time lag  $\Delta t$  is processed using an analog method. The contrast detection abilities of the LMD depend largely on the bandwidth of the analog band-pass filter.

Figure 2 illustrates the advantages of the temporal derivative of the photosensor signals in the motion detection preprocessing step. We now take the case where the pair of photosensors depicted in Figures 1 and 2 turns at a *variable angular speed*  $\Omega$ . In Figure 2b, for example, let us assume that  $\Omega$  decreases exponentially during a clockwise rotation from its present position towards  $\psi(t) = 0$ . Speed  $\Omega$  will be higher when the segment is in position 1 than in position 2. Hence the LMD output, which reflects the angular speed  $\Omega$ , will gradually decrease when the abscissa of segment AB increases.

### 4. Hardware implementation of the variable speed scanning

We built an elementary scanner, the components of which are sketched in Figure 3. A lens (focal length : 8mm) and a dual photosensor mounted opposite each other on a blackened perspex drum, formed a miniature "camera eye", which was driven by a DC micromotor (diameter 10mm). The angular position of the drum (and hence that of the sensor's visual axis) was measured by means of a magnetoresistive sensor responding to the angular position of a micromagnet glued to the hub of the drum. A position-servomechanism made it possible for the visual axis of this elementary eye to follow a reference signal.

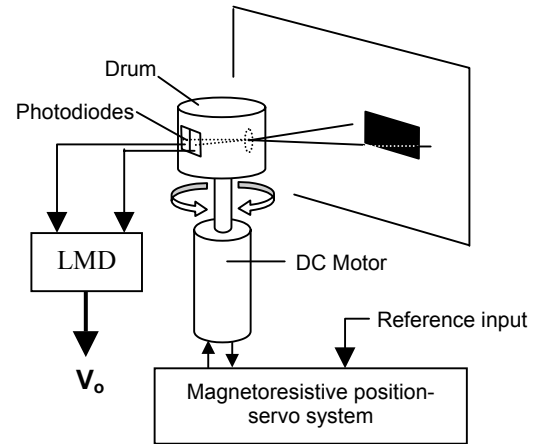


Fig. 3 Sketch of the complete scanning sensor

Taking the motor's parameters and the sensor's sensitivity into account (Table1), the dynamic response of this servo-system was tuned via a lead compensator such that the phase margin was  $60^\circ$  at a frequency of 80Hz.

Motor	Magnetoresistive sensor
Reduction ratio : 64	1.8 mV/ $^\circ$
Mechanical time constant : $9 \cdot 10^{-3}$ s	
Electrical time constant : $7.5 \cdot 10^{-7}$ s	

Table 1 Motor and angular sensor parameters

A variable speed was obtained simply by filtering a rectangular input signal via a passive first-order low-pass filter. The resulting signal (Figure 4a) served as the reference input to the position-servo system and yielded a quasi-exponentially varying angular speed  $\Omega$ . Figure 4b shows the motor input and Figure 4c shows the resulting angular orientation of the "eye" as monitored by the magnetoresistive sensor.

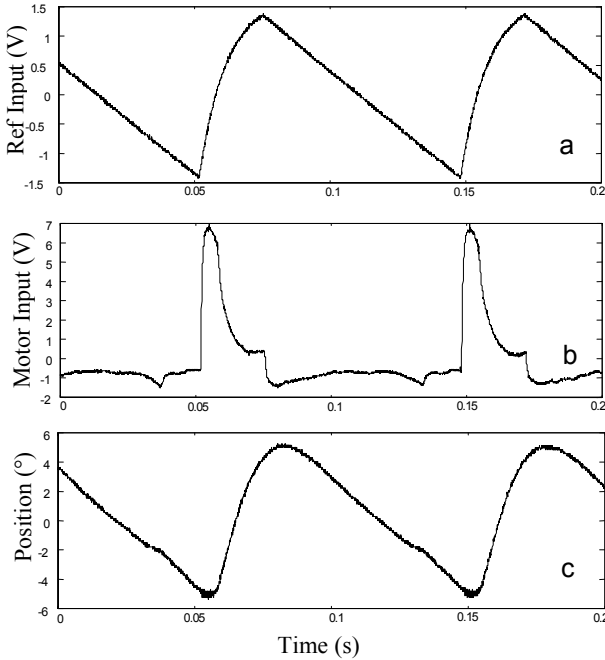


Fig. 4 Signals from the position-servo

## 5. Performance of the variable speed scanner coupled to the LMD

Like many fly motion detecting neurons [4], the analog LMD is directionally selective. Since it responds only to a single scanning direction, we produced a scanner performing dissymmetric scanning with a long phase (100ms from  $4^\circ$  to  $-4^\circ$ ), during which the LMD did not respond, followed by a shorter "return phase" (25ms from  $-4^\circ$  to  $4^\circ$ ), during which motion detection was effective. The total scan period was therefore 125ms. The amplitude of the scan is characterized by the scanning factor  $\alpha$  [8] given by:

$$\alpha = \frac{\Delta\xi}{\Delta\phi}$$

where  $\Delta\xi$  is the angular amplitude of the scan. In the present case, we took  $\alpha = 2$ . The scanning sensor was mounted onto a precision rotary table in order to vary the orientation  $\phi_c$  of the "eye" in relation to the contrasting object in the visual field (Figure 5). The object was a

contrast step made of grey paper that stood out from the background. The contrast  $m$  was determined by measuring the relative illuminance of the paper ( $I_1$ ) and its background ( $I_2$ ) and calculating  $m = \frac{I_1 - I_2}{I_1 + I_2}$ . Contrast

was measured *in situ* with a linear photo device having the same spectral sensitivity as the dual photosensor used.

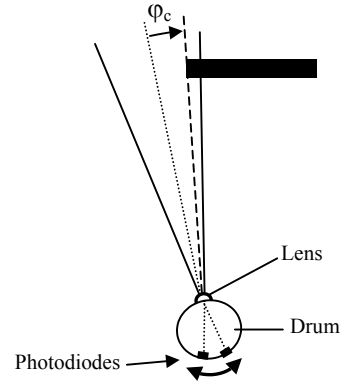


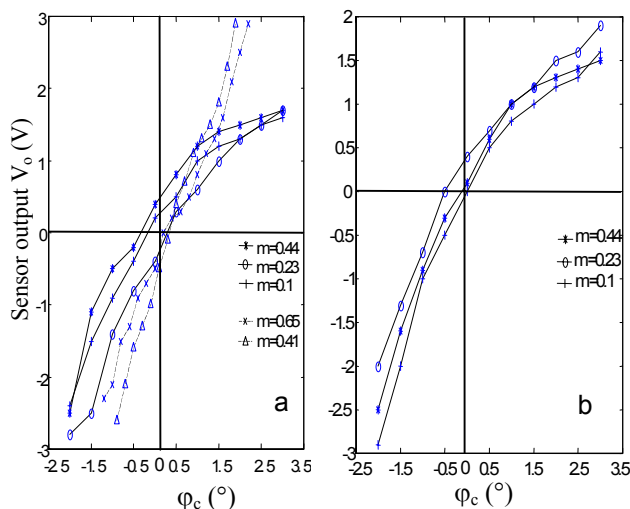
Fig. 5 Orientation  $\phi_c$  of the eye with respect to the contrast edge.

Figure 6 shows that during the "working phase" of the scan, the LMD gave an output which varied with the angular position of the contrasting object within the sensor's visual field. This response has two particularly interesting aspects:

- it is quasi-linear with respect to the angular position  $\phi_c$
- it is largely invariant with respect to the contrast  $m$  of the object and distance.

These two aspects are as welcome as they are unusual in a non-contact sensor, because they open the way to using this scanning sensor in an optomotor control loop for stabilizing a system subject to rotational drifts, with respect to a stationary object, regardless of its level of contrast. This control loop can also perform angular tracking on a remote object provided the resulting angular speed is sufficiently low (a higher scanning frequency would cope with a faster angular drift).

The scanning sensor complete with its control system and LMD was constructed using SMD technology. It has a diameter of 50mm and a total weight of 30g. The measurements shown in Figure 6 were performed with a maximum sensor-to-object distance of 1.4m. At this distance, the minimum detectable contrast was 10%. A good signal-to-noise ratio was obtained by adapting the filtering properties of the processing stages of the LMD to the scanning frequency. Note that the only strict requirement is that a contrast edge should be present in the environment.



**Fig. 6** Voltage output from the scanning sensor as a function of its orientation  $\varphi_c$  with respect to a dark edge (solid) and a dark stripe 10mm in width (dotted), at various contrast values  $m$  and distances :  $D=60\text{cm}$  (a) and  $D=140\text{cm}$  (b),  $\alpha = 2$ . Accuracy:  $\pm 0.05^\circ$ . Resolution:  $0.05^\circ$ .

## 6. Conclusion

Subsequent to the development of other biologically-inspired retinal scanners that were used to guide mobile robots [8][9], we have now designed and constructed a new type of visual sensor, which combines motion detection with scanning at variable speed. This scanning sensor is a non-contact, non-emitting device that surveys a small part of the visual environment, within which it is able to measure the angular position of a contrast feature with a high resolution. Interestingly, this sensor manages to measure a position on the basis of a speed measurement.

This sensor, which is small-sized, low-weight, low-complexity and low cost ( $\cong 400$  USD), displays two essential properties (Figure 6) :

- its output signal varies in a quasi-linear fashion with the angular position of a contrast edge in its field of view.
- its output is largely independent of the distance and the level of contrast involved.

These are valuable properties when it comes to incorporating the sensor into an optomotor loop in order to achieve accurate angular stabilization of a sensory platform subject to yaw, pitch, or roll with respect to a stationary environment [11]. The variable speed scanning principle is well adapted to MOEMS technology (e.g. micro mirror scanner), which would significantly decrease the size of the sensor.

## Acknowledgments

We thank M. Boyron for his expert technical assistance and I. Daveniere and J. Blanc for improving the English

manuscript. This research was supported by CNRS (Life Sciences, Engineering Sciences, GIS Cognisciences and Programme on Microsystems). S. Viollet received a predoctoral fellowship from Ministry of National Education and Scientific Research (MENRS).

## References

- [1] E. Buchner, "Behavioural Analysis of Spatial Vision in Insects," *In: Photoreception and vision in Invertebrates*, Vol. 74, pp. 561-621, Ed. M. A. Ali, New York, 1982.
- [2] T. Collett, and H. Nalbach, H. Wagner, "Visual stabilization in arthropods," *In: Visual Motion and its role in the Stabilization of Gaze*, Vol. 11, pp. 239-263, Ed. Elsevier, 1993.
- [3] N. Franceschini, and R. Chagneux, "Repetitive scanning in the fly compound eye," *Proc Göttingen Neurobiology Conf*, 1997.
- [4] N. Franceschini, and A. Riehle, A. Le Nestour, "Directionally Selective Motion Detection by Insect Neurons," *Facets of Vision*, pp. 360-390, Eds Stavenga & Hardie, Springer, Berlin, 1989.
- [5] N. Franceschini, J. M. Pichon, and C. Blanes, "From insect vision to robot vision," *Phil Trans Roy Soc Lond B*, Vol. 337, pp. 283-294, 1992.
- [6] R. C. Hardie, "Functional organisation of fly retina," *In Progress in Sensory Physiology*, Vol. 5, pp.1-79, Ed. D. Ottoson, Springer, Berlin, 1985.
- [7] S. Laughlin, "Form and function in retinal processing," *TINS*, Vol. 10, pp. 478-483, 1987.
- [8] F. Mura, and N. Franceschini, "Obstacle avoidance in a terrestrial mobile robot provided with a scanning retina," *Proc Intelligent Vehicles*, Vol. 2, pp. 47-52, Eds M. Aoki and I. Masaki, Tokyo, 1996.
- [9] F. Mura, and I. Shimoyama, "Visual Guidance of a Small Mobile Robot Using Active, Biologically-Inspired, Eye Movements," *Proc IEEE R&A*, pp. 1859-1864, Leuven, 1998.
- [10] J. C. Radix, *Gyroscopes et Gyromètres*, Ed. Cepadues, Toulouse (France), 1997.
- [11] S. Viollet, and N. Franceschini, "Visual servo system based on a biologically-inspired scanning sensor," *Sensor Fusion and Decentralized Control in Robotic Systems II Conf*, SPIE Photonics East, In press, Boston, 1999.